Hindawi Publishing Corporation
ISRN Mechanical Engineering
Volume 2013, Article ID 521375, 12 pages
http://dx.doi.org/10.1155/2013/521375

Research Article

Modeling of Homogeneous Mixture Formation and Combustion in GDI Engine with Negative Valve Overlap

M. K. Lalith, Akshay Dinesh, S. Unnikrishnan, Akhil Radhakrishnan, S. Srihari, and V. Ratna Kishore

Department of Mechanical Engineering, Amrita Vishwa Vidyapeetham, Coimbatore 641112, India

Correspondence should be addressed to V. Ratna Kishore; v_ratnakishore@cb.amrita.edu

Received 31 July 2013; Accepted 27 August 2013

Academic Editors: F. Liu and Z. Yu

Mixture homogeneity plays a crucial role in HCCI engine. In the present study, the mixture homogeneity was analysed by three-dimensional engine model. Combustion was studied by zero-dimensional single zone model. The engine parameters studied include speed, injector location, valve lift, and mass of fuel injected. Valve lift and injector location had less impact on mixture formation and combustion phasing compared to other parameters. Engine speed had a noticeable effect on mixture homogeneity and combustion characteristics.

1. Introduction

Over the last decade, we have seen an exponential growth in the consumption of diesel and petrol by automobiles. This has contributed a great deal in air pollution. Hence, it is important to use the right technology to harness maximum output from the fuel and at the same time, reduce pollutions. Homogenous charged compression ignition (HCCI) engine is a mix of both conventional spark-ignition and diesel compression ignition technology. The combination of these two designs offers diesel-like high efficiency and at the same time, reduces NO_x and particulate matter emissions. HCCI simply means that the fuel is homogeneously mixed with air in the combustion chamber (very similar to a regular spark-ignited gasoline engine), but with a very high proportion of air to fuel (lean mixture). Currently, lots of researches are being done on challenges faced to operate an engine in HCCI mode; some of them are mixture homogeneity, combustion phasing, and limited operating range. Among these, mixture homogeneity at the end of compression stroke plays a crucial role in implementing HCCI successfully [1]. Various modeling strategies have been used to study combustion in HCCI gasoline engines, which include zero-dimensional single zone [2, 3], quasidimensional multizone [4], one-dimensional cycle simulation coupled with chemical kinetics model [5–7], multidimensional multizone [8–11], and multi-dimensional with detailed chemistry [12–16]. Multi-dimensional modeling provides high levels of accuracy but at the cost of computational time.

Xu et al. [3] developed a single zone combustion model based on detailed chemical kinetics combined with a thermodynamic engine simulation program. It was found that the main combustion, marked by the rapid increase of temperature, starts in the temperature range of 1000–1050 K. Roy and Valeri [11] devised a multi zone model with a detailed chemistry approach. The results demonstrated that the separate combustion zones predict well the cylinder pressure history and the rate of heat release, as well as the moment of auto-ignition and the peak pressure. Kontarakis et al. [17] performed experiments to obtain HCCI mode in a four-stroke SI engine with a compression ratio of 10.3 by modifying the valve timing. Stable conditions for using HCCI were found to be 2.5–3.6 bar IMEP and 1300–2000 rpm. Moreover, in HCCI, combustion was fast, and the duration of crank angle was almost constant. Kong et al. [15] developed a CFD model with detailed chemistry. It was found that optimization of NO_x and UHC can be achieved by controlling the intake temperature together with the start-of-injection timing. Kong and Reitz [16] extended their work; the effects of flow turbulence on HCCI engine combustion by using different piston geometries were investigated. Results showed that the combustion duration in square bowl is longer than

flat piston case because of more turbulence. Tain et al. [18]. and Li et al. [19] studied HCCI ignition timing and heat release rate by using multistage injection and negative valve overlap (NVO) using zero dimensional model. The first stage which involves injection of fuel during negative valve open period leads to the formation of active species which will improve ignition properties. The second stage characterised by early injection can provide HCCI condition because of the sufficient time available for mixing.

It can be observed that most of the previous works use multi zone/single zone zero dimensional model to study the performance of HCCI engines. These models cannot predict homogeneity of mixture formation. To study mixture formation, the three-dimensional model is the most preferred model, as it can produce more realistic results. The combustion model can be zero-dimensional model to get approximate results as the computational time increases for three dimensional modeling for combustion. This present work studies the effect of various engine parameters on homogeneity of mixture formation using three-dimensional engine model. Also, the combustion analysis was done using zero-dimensional single zone model with detailed reaction mechanism.

2. Modeling Methodology

CONVERGE is used for the three-dimensional CFD modeling. The equations of conservation of mass, momentum, turbulence, and energy are solved. Governing equations are given elsewhere [20].

Control-volume-based technique was used to convert the governing equations to algebraic equations that can be solved numerically. The second-order upwind scheme was used for spatial discretization of all the governing equations. The PISO algorithm is used for pressure and velocity coupling. Pressure interpolation of the pressure values at the faces is done using momentum equation coefficients (standard pressure interpolation scheme). The double-precision segregated solver was utilized with implicit method for solving the discretized set of algebraic equations.

2.1. Computational Domain and Gridding. The present study uses three dimensional engine geometry as it can predict realistic results. The surface file was imported into CONVERGE and different boundaries faces were grouped as shown in Figure 1.

The specifications of the engine used for the simulations are given in Table 1. The valve timing was taken from [20] so as to get negative valve overlap, and it is given in Table 2. The injection parameters were taken from [20], and it is given in Table 3. Figure 2 shows the dual injection timing in a P-θ plot.

In CONVERGE, the grid is generated run-time. Base grid size has to be specified, and there are three main ways of manipulating the grid size further. The grid is easily coarsen or refined by using the grid scaling feature which adjusts the base grid size. Secondly, the grid with a fixed or time-dependent refinements (embedding) is configured when and where it is needed. Finally, Adaptive Mesh Refinement (AMR) can be used to add grid refinement in critical areas of domain based on the solution variables. These parameters were then optimised for computational time and to attain grid independent results. Figure 3 shows a mesh slice generated during simulation. It can be observed that the mesh is finer around the valve as the velocity gradients are very high during the valve opening. The boundary embedding given to the piston can also be seen in Figure 3.

2.2. Initialisation and Boundary Condition. The various physical quantities were initialized with quantities which resemble

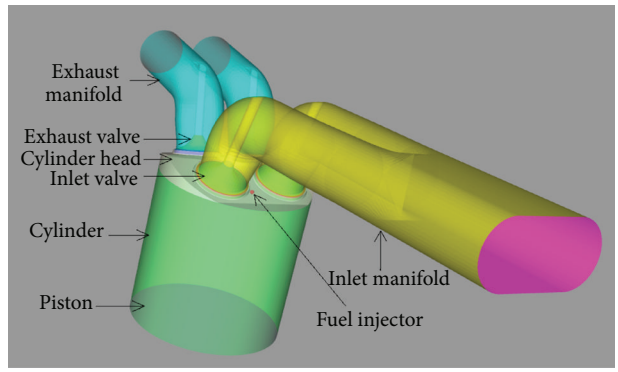

Figure 1: Three dimensional engine model with various boundaries.

Table 1: Engine specification.

Bore × stroke	0.1016 m × 0.10 m
Compression ratio	13
Connecting rod length	0.18 m
Piston geometry	Flat piston
Injection pressure	5 MPa
Injection temperature	450 K

Table 2: Port timing.

EVO bBDC	44°
EVC aTDC	58°
IVO bTDC	64°
IVC aBDC	24°

Table 3: Injection parameters.

	Case 1	Case 2
Injection pressure	5 MPa	5 MPa
Injection temperature	335 K	335 K
Spray cone angle	54°	54°
	Pilot injection (I_1)	
Mass	1.25 mg	0.8 mg
Start of injection	30 BTDC	30 BTDC
Duration	1.211°CA	0.766°CA
	Main injection (I_2)	
Mass	11.25 mg	7.2 mg
Start of injection	100° ATDC	100° ATDC
Duration	10.899°CA	6.976°CA

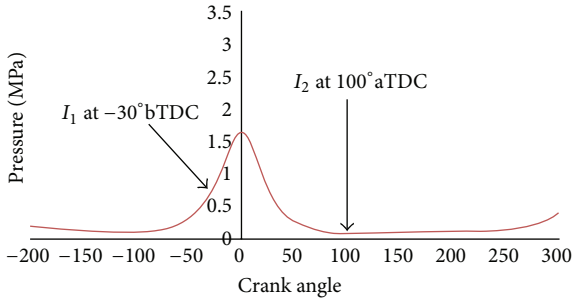

Figure 2: Pressure plot showing two injection timings.

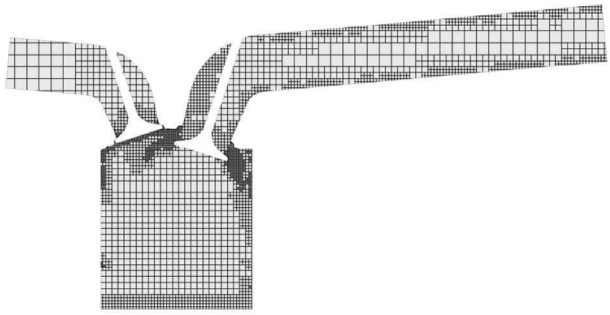

Figure 3: Mesh slice generated during the simulation with embedding and AMR.

real engine condition. The simulation was a single-cycle simulation. Hence, to get the initial conditions inside the cylinder, complete combustion of the fuel was assumed, and the resulting species mass fractions were found out using STAJAN [21]. The burnt gas temperature was assumed as 90% of adiabatic flame temperature. The pressure and temperature at the end of expansion stroke were found out by assuming adiabatic expansion. Then, these values were initialised in the combustion chamber. At the inlet port, the temperature of air was taken as 300 K, and the pressure was taken as atmospheric pressure. At exhaust port, the temperature of air was taken as 700 K, and the pressure was taken as atmospheric pressure.

In order to solve the governing transport equation, a boundary condition for each equation must be specified. The inlet valve, exhaust valve, and piston are moving wall boundaries. Cylinder, cylinder head, and ports are fixed wall boundaries. The inlet of inlet port is inflow boundary condition, where, pressure is specified. The outlet of exhaust is outflow boundary condition, where pressure is specified.

3. Results and Discussion

3.1. Mixture Analysis. Mixture homogeneity plays an important role in HCCI engine. Mixture formation was analysed by varying speed, amount of fuel, injector location, and valve lift. The mixture formed at 20° CA BTDC in compression stroke was studied, because usually in an engine, combustion phasing happens before TDC. The simulation starts at 50°bBDC in expansion stroke. The simulation ends at 20°bTDC in compression stroke.

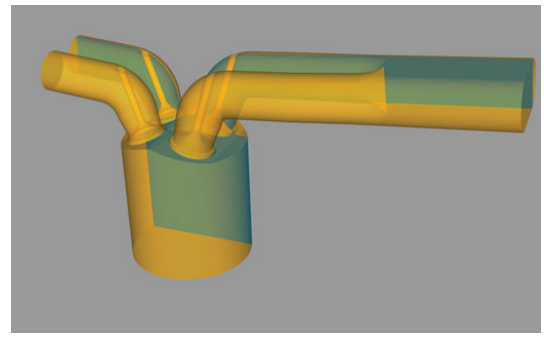

Figure 4: The clip plane used in the study.

Two-valve lifts were considered in this study. The first valve lift had a maximum lift of 3.45 mm. Whereas, the second valve lift had a maximum lift which was 1.5 times the maximum lift of the first valve lift, that is, 5.175 mm. The first valve lift was referred as "x", and the second valve lift was referred as "1.5x". This convention is used throughout the paper. Two injector locations were taken into account in this study, namely, side injection (as shown in Figure 1) and central injection (injector at geometric center of cylinder head). Figure 4 shows the clip plane which we consider in this study. The clip plane is at a distance of $1.9091e-2$ m from the geometric center of the cylinder.

3.1.1. Effect of Speed. The effect of various speeds on mixture formation is dealt with in this section. Engine speeds taken into account were 1000 rpm, 1500 rpm, and 2000 rpm. The other parameters which were kept constant includes valve lift "1.5x", amount of fuel injected was 12.5 mg, and side injector for all the cases. The contours of isooctane mass fractions formed at 20°bTDC for various speeds are shown in Figure 5.

It can be observed from Figure 5 that 1500 rpm formed better homogeneous mixture than both 1000 rpm and 2000 rpm cases. A one thousand rpm had a small pocket of inhomogeneity near the inlet valve, whereas 2000 rpm had a small pocket of inhomogeneity near the exhaust valve. The mixture formation at 20°bTDC can be explained by plotting velocity vector along with the contours of isooctane mass fractions before the piston reached top dead centre. Two crank angles were selected for this purpose, 10°bBDC which is just before intake valve closing, and 90°aBDC which is half-way through the compression stroke. The contours of iso-octane mass fraction along with the velocity vectors for different speeds are shown in Figure 6.

Mixture homogeneity is controlled by two factors, namely, direction and magnitude air velocity and fuel vaporisation. From Figure 6, it can be observed that the orientation of air was similar, but the magnitude of velocity vector increases as the engine speed increases. It was also noted that at 90°aBDC, the air velocity was not enough to complete the mixing of fuel in 1000 rpm case. In case of 1500 rpm, the air velocity was sufficient enough to distribute the mixture homogeneously. For 2000 rpm, the velocity of air was more than required which resulted in a small inhomogeneity.

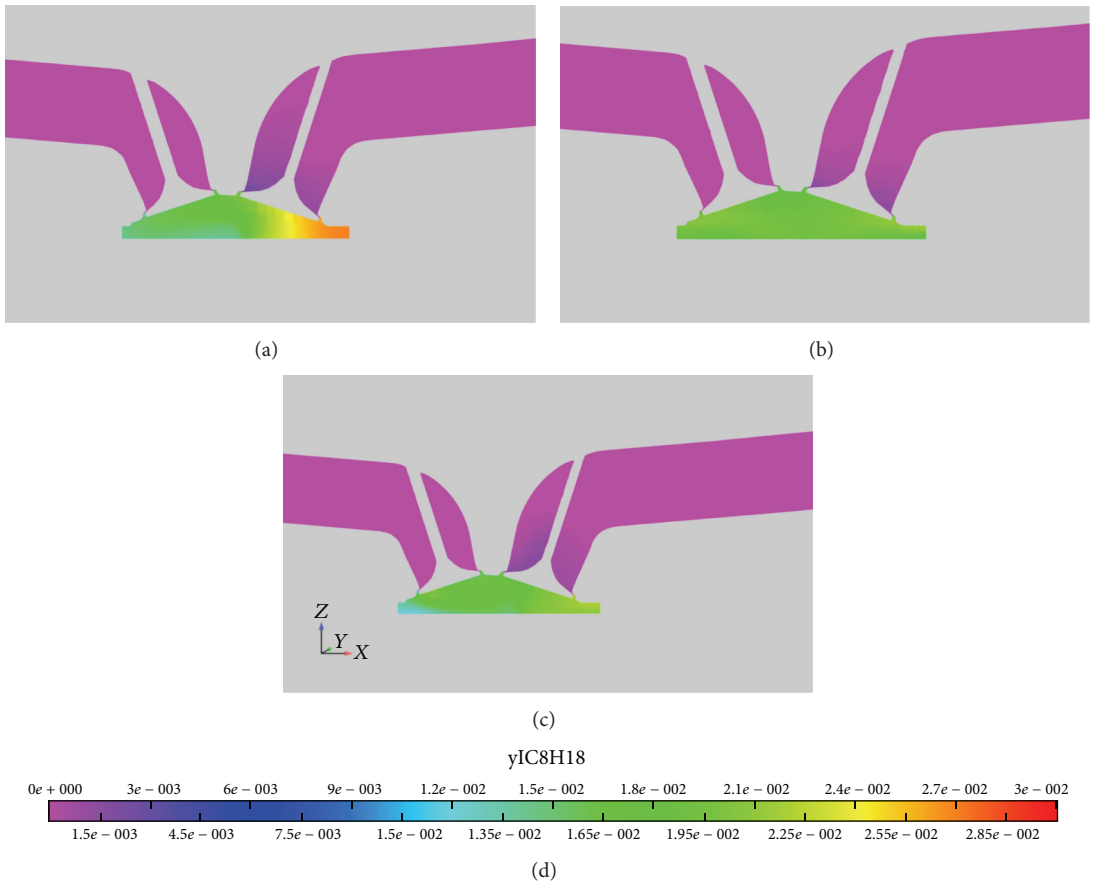

Figure 5: Contours of iso-octane mass fractions at 20°bTDC in compression for (a) 1000 rpm, (b) 1500 rpm, and (c) 2000 rpm.

Figure 7 shows the T-ϕ plots inside the combustion chamber for the three cases.

From Figure 7, it can be observed that all the cases were almost homogeneous. Among the three, 1500 rpm had a narrow band when compared to 1000 and 2000 rpm. This indicates that 1500 rpm formed better homogeneous mixture than other two speeds.

3.1.2. Effect of Loading. In this section, the effect of loading in mixture formation is studied. Two quantities of fuel were selected. They were 8 mg and 12.5 mg. The other parameters were kept constant. Engine speed was 1500 rpm, valve lift was "1.5x", and side injector location was selected. The contours of iso-octane mass fractions formed at 20°bTDC are shown in Figure 8.

It was observed from Figure 8 that 8 mg forms comparatively lean mixture than 12.5 mg on an average because of its amount of fuel for the given volume. The velocity vectors along with iso-octane mass fraction contours at 10°bBDC and 90°aBDC are shown in Figure 9.

From Figure 9, it was observed that velocity profile is almost the same, since engine speed is kept constant. Only difference occurs in the magnitude of mass fraction, as 8 mg fuel loading would form a leaner mixture. Thus, it can be concluded that regardless of the amount of fuel injected, the mixture formed will be almost homogeneous before combustion.

3.1.3. Effect of Injector Location. This section deals with the effect of injector location on mixture formation. Two injector locator locations were selected to study the effect of injector location in mixture formation. They were side injection and centre injection. The other parameters were kept constant. Valve lift was "x", amount of fuel injected was 12.5 mg, and engine speed was 1500 rpm for both cases. The contours of iso-octane mass fractions for two injector locations are shown in Figure 10.

It was observed from Figure 10 that both the cases formed near homogeneous mixture. But, were the central injection case produced better homogeneity than side injection. The contours of iso-octane mass fractions along with velocity vectors at 10°bBTC and 90°aBDC are shown in Figure 11 which, can be used to explain this trend.

From Figure 11, it was observed that velocity vectors were almost the same for both conditions as engine rpm for both cases was the same. The only difference was the position of fuel injector. It can be noted that, at 90°aBDC, the fuel was more concentrated at the corners of the combustion chamber. As the compression stroke was completed, the air could not distribute the fuel uniformly. Thus, pockets of high

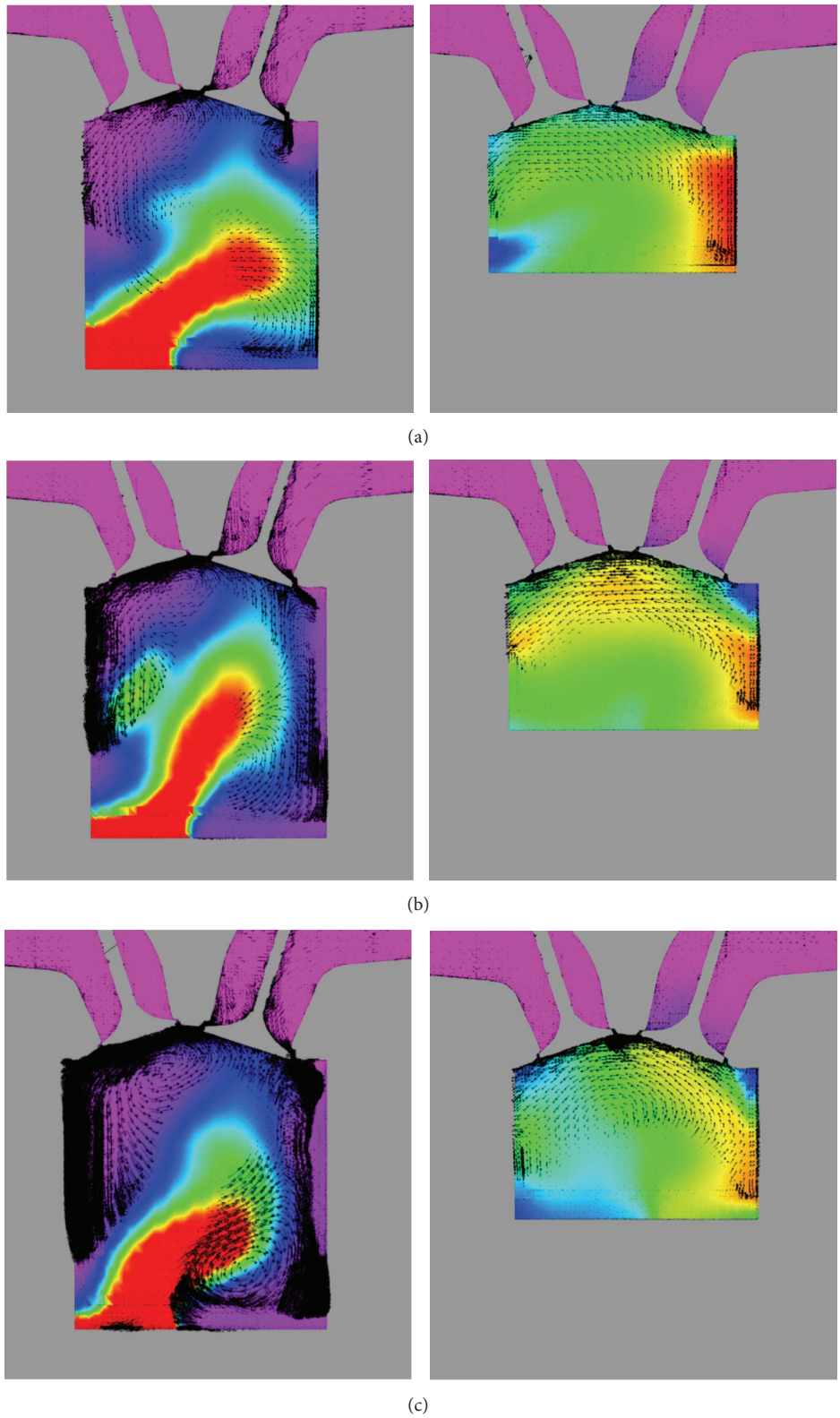

(a)

(b)

(c)

Figure 6: Contours of iso-octane with velocity vector at 10°bBDC (left) and 90°aBDC (right) for (a) 1000 rpm, (b) 1500 rpm, and (c) 2000 rpm.

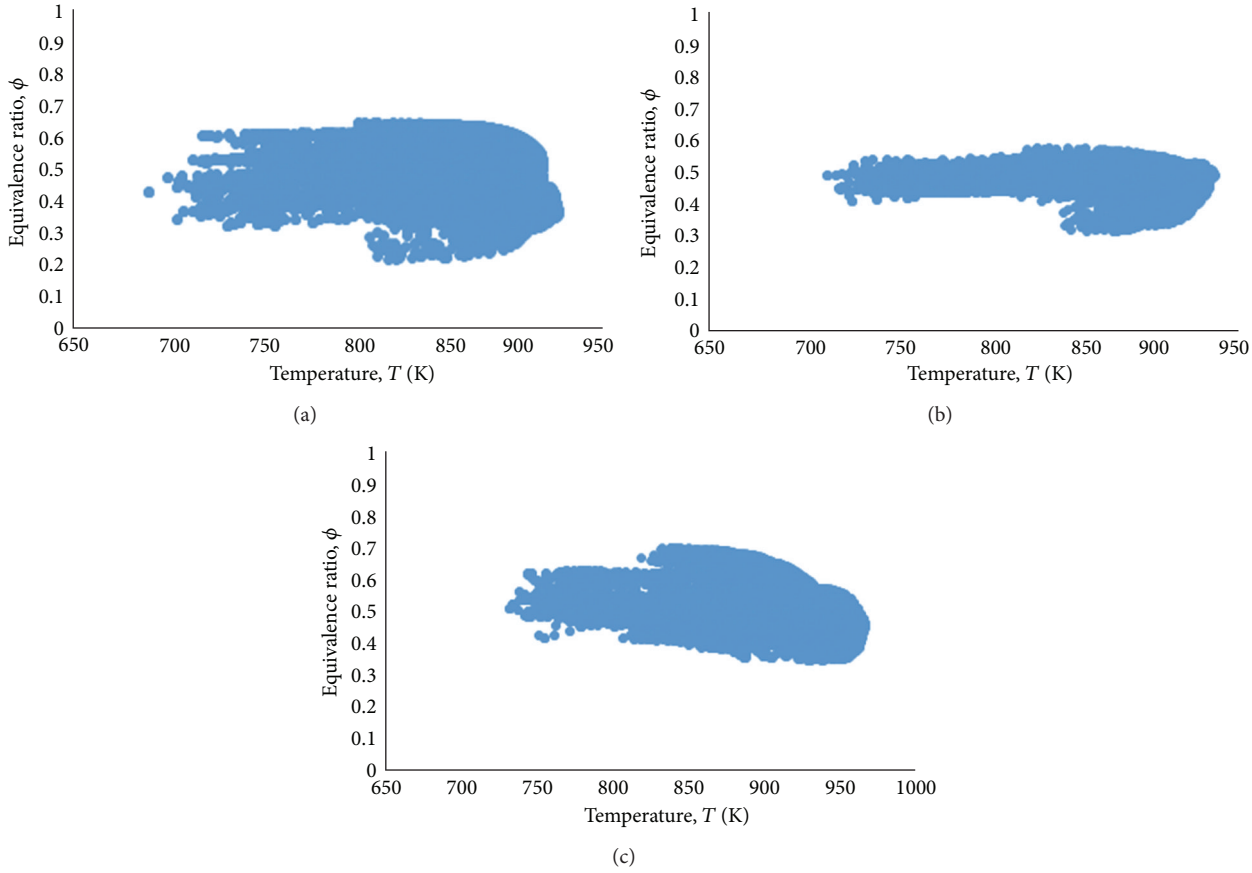

FIGURE 7: T-ϕ plots inside the cylinder for (a) 1000 rpm, (b) 1500 rpm, and (c) 2000 rpm at 20° CA bTDC in compression stroke.

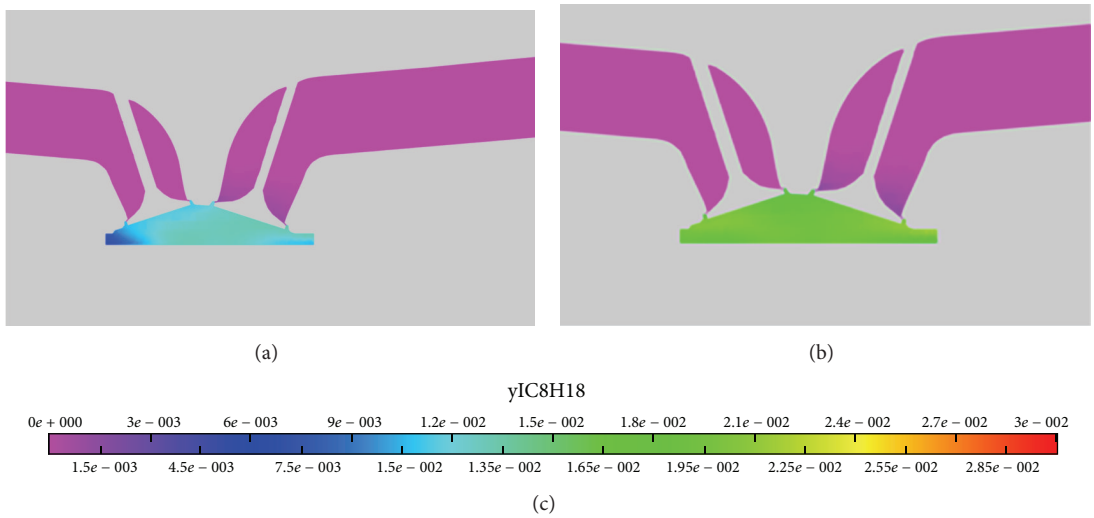

FIGURE 8: Contours of iso-octane mass fractions at 20°bTDC for (a) 8 mg fuel and (b) 12.5 mg fuel.

concentrations of iso-octane were formed in these corners. It can also be noted that central injection case formed better homogeneous mixture than side injection case.

3.1.4. Effect of Valve Lift. In this section, the effect of valve lift on mixture formation is studied. The most common way of attaining negative valve overlap (NVO) is by reducing the valve lift, thereby reducing the overall opening time of the valve. Two-valve lifts considered in this study were "x" and "1.5x". The other parameters were kept constant. Amount of fuel injected was 12.5 mg, engine speed was 1500 rpm, and side injector location was selected. The contours of iso-octane

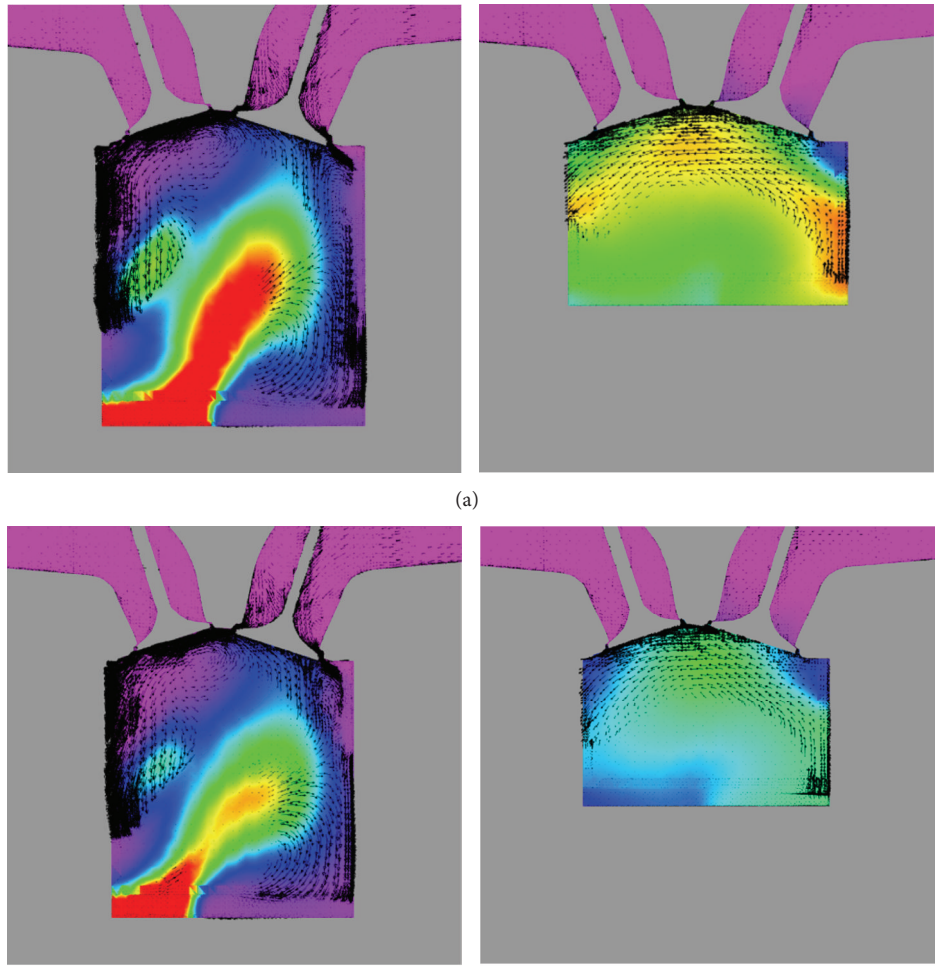

(a)

(b)

Figure 9: Contours of iso-octane mass fractions with velocity vectors at 10°bBDC (left) and 90°aBDC (right), (a) 12.5 mg and (b) 8 mg.

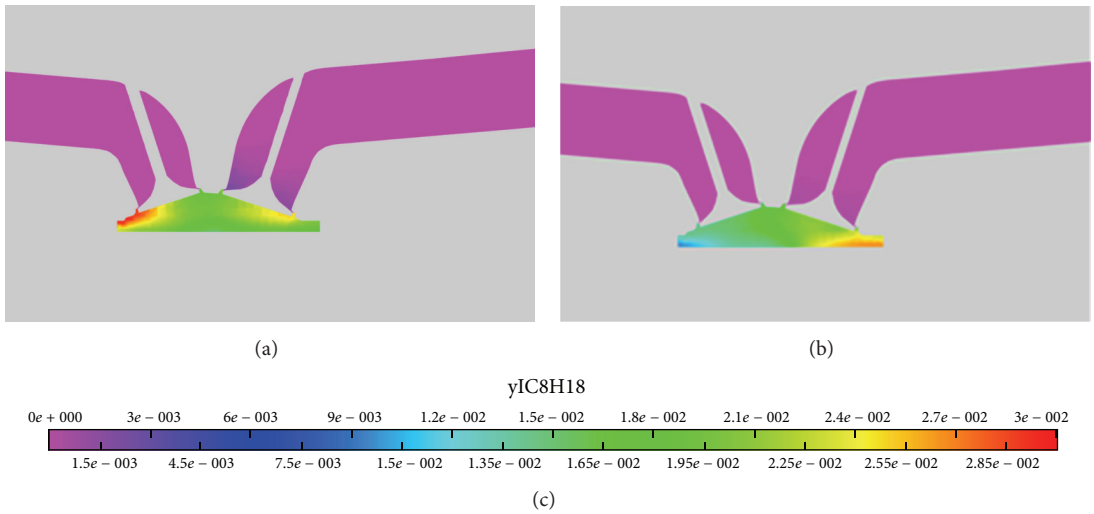

(a) (b)

(c)

Figure 10: Contours of iso-octane formed at 20°bTDC for (a) side injection and (b) central injection.

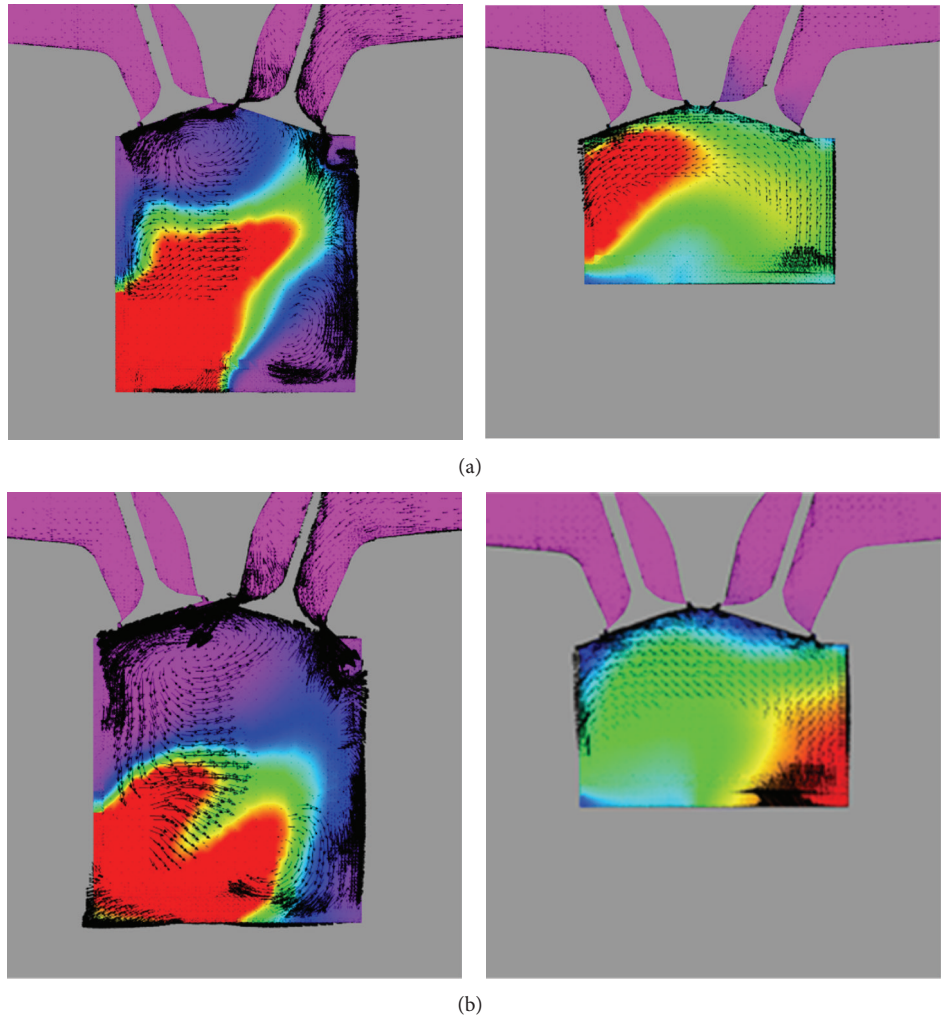

FIGURE 11: Contours of iso-octane mass fractions with velocity vectors at 10°bBDC (left) and 90°aBDC (right), (a) side injection and (b) central injection.

mass fractions at 20°bTDC for two-valve lifts are shown in Figure 12.

Figure 12 shows how the mixture formation varies with change in valve lift. Figure 13(a) shows the mixture formed, where the valve lift is increased by 50%. It was observed that for 1.5x, valve lift forms much more homogenous charge compared to "x". The contours of iso-octane mass fractions along with velocity vectors at 10°bBTC and 90°aBDC are shown in Figure 13.

From the Figure 13, it was observed that the velocity vectors tend to move the fuel from higher concentration to lower concentration in "1.5x" case than "x" case. Hence inhomogeneity is higher in "x" case.

3.2. Combustion Analysis. CHEMKIN was used for combustion analysis with zero-dimensional modeling. A reaction mechanism of gasoline with 1300 species was used [22]. The input variables for CHEMKIN which include mixture composition, in-cylinder pressure, and mean temperature were taken from CONVERGE at 20° BTDC in the compression stroke. The mixture was nearly homogeneous. The heat release rate and pressure, were studied to understand the effect of various engine parameters.

3.2.1. Effect of Speed. Engine speed was varied to find its effect on the combustion phasing. The speeds considered were 1000, 1500, and 2000 rpm. The valve lift in all the cases was kept as 1.5x. The amount of fuel was kept constant at 12.5 mg. Figures 14 and 15 show the heat release rate per crank angle for different speeds and P-θ curves, respectively.

It was observed from Figure 14 that for higher speeds, heat release peak tends to decrease and shift after TDC compared to lower speeds. The shifting of peak can be attributed to ignition delay and hence, results in late combustion. The reduction in peak could be because of volume expansion as combustion occurs after TDC, and hence, lower heat release rates are obtained for lower engine speeds.

From Figure 15, it was found, at 356° crank angle for 1000 rpm, there was a sudden rise in pressure curve; this could be attributed to the sudden heat release inside the

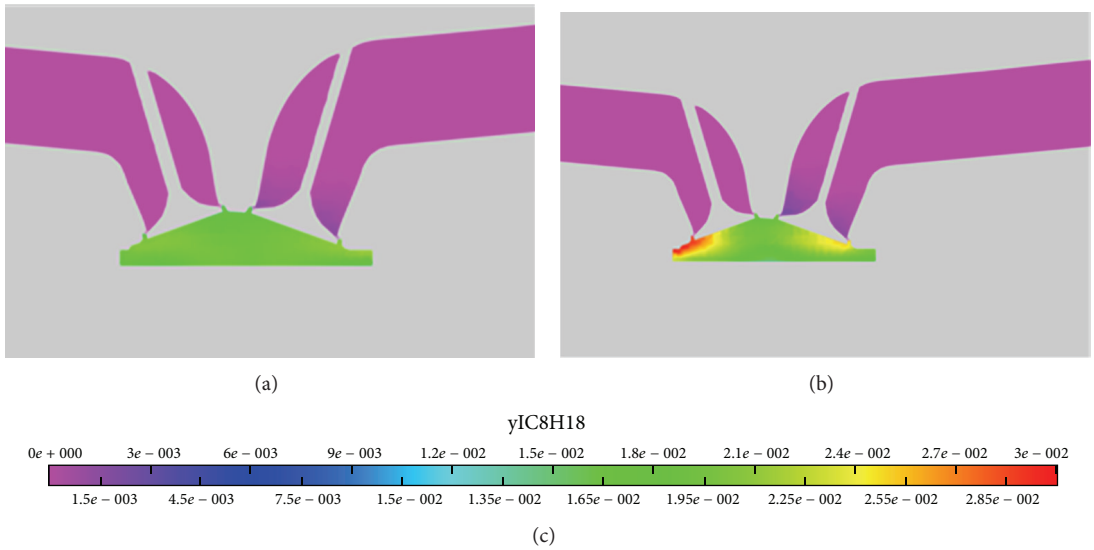

Figure 12: Contours of iso-octane mass fractions at 20°bTDC (a) 1.5x valve lift and (b) x valve lift.

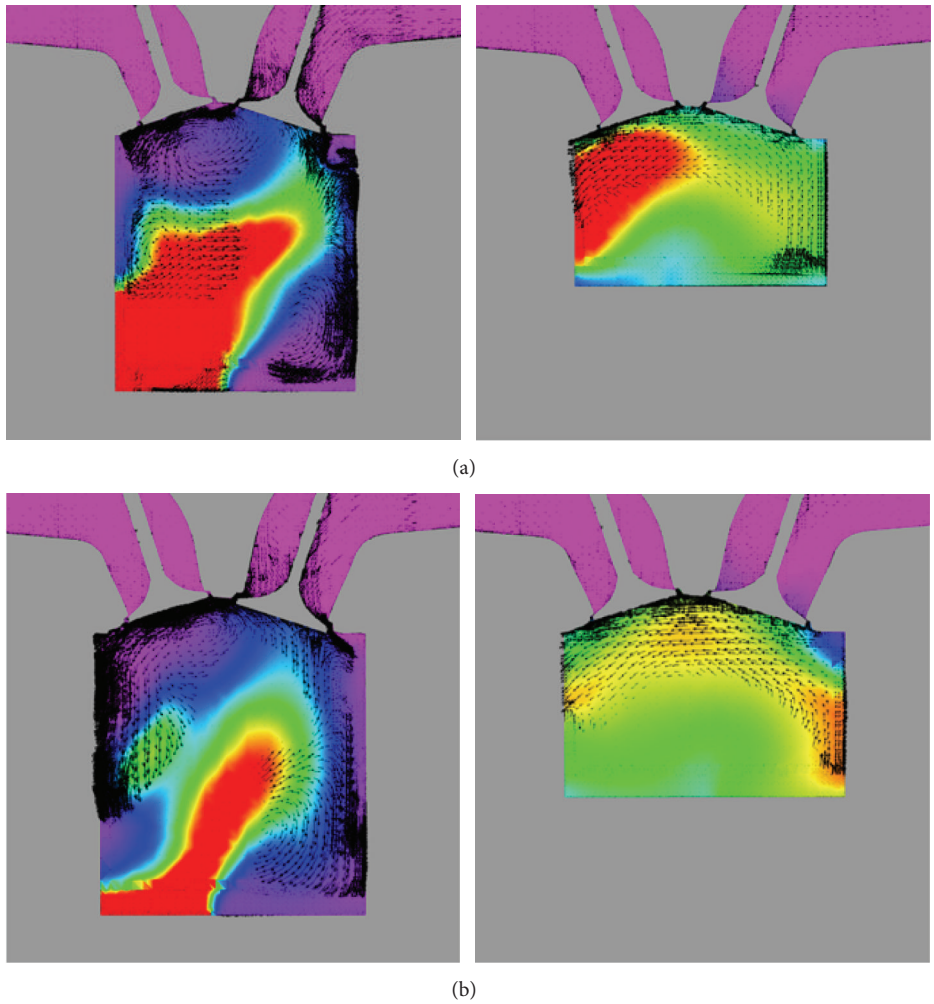

Figure 13: Contours of iso-octane mass fractions with velocity vector at 10°bBDC (left) and 90°aBDC (right) for (a) x valve lift and (b) 1.5x valve lift.

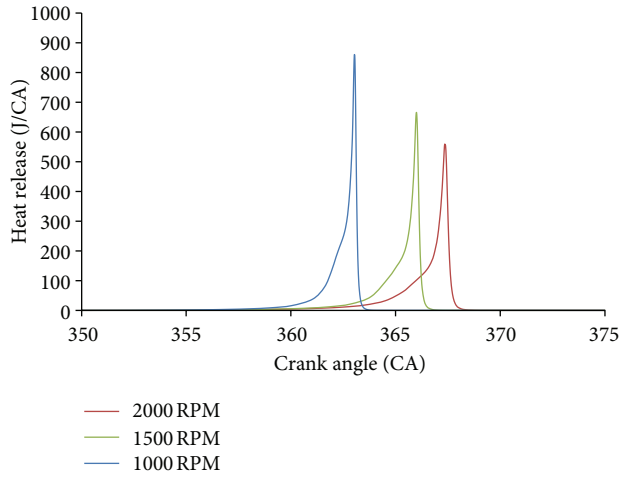

Figure 14: Heat release plots for different speeds.

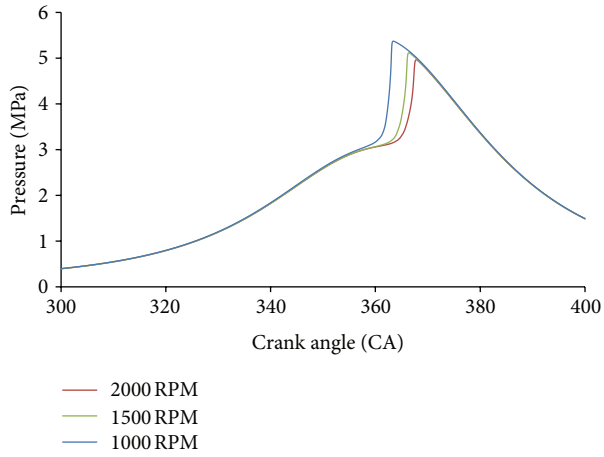

Figure 15: P-θ curve for different speeds.

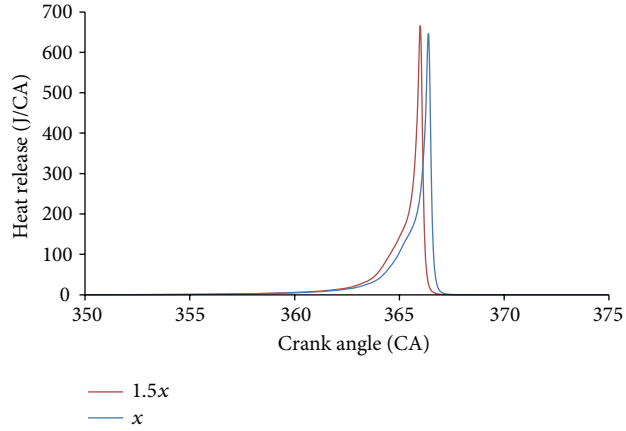

Figure 16: Heat release plots for x and 1.5x.

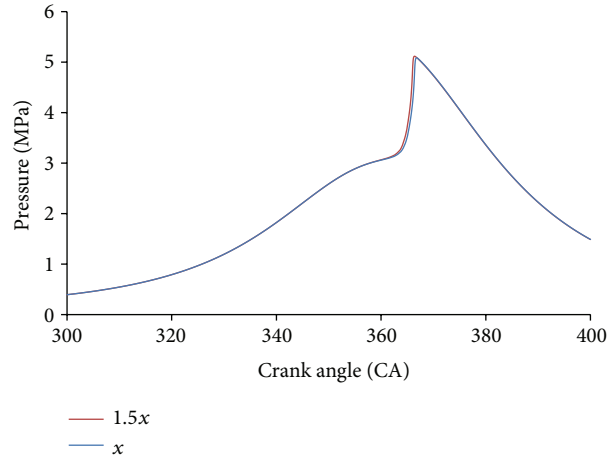

Figure 17: P-θ curve for x and 1.5x.

combustion chamber. Moreover, for higher speed, the peak pressure tends to decrease. This might be due to the fact that at higher speeds, the heat release rate reduces.

3.2.2. Effect of Valve Lift. In this section, the effect of valve lift in combustion phasing is studied. The effects of valve lift x and 1.5x were studied. The speed was kept constant at 1500 rpm and the amount of fuel injected was 12.5 mg for both cases. The heat release curve thus obtained is shown in Figure 16, and the P-θ curve is shown in Figure 18.

The heat release rate curves showed negligible variations in heat release peaks. However, heat release peak for 1.5x was fractionally more, mostly because of the fact that slightly more air was available for combustion inside the cylinder. The reason for negligible variation can be attributed to the fact that though the valve lift is increased, the effective valve opening time is the same.

The pressure curves shown in Figure 17 for two different configurations, namely x and 1.5x, were plotted and it was found that the deviations were minimal. The primary reason could be because of negligible difference in heat release curves as shown in Figure 16.

3.2.3. Effect of Injector Location. The effect of injector location in combustion phasing is dealt with in this section. Two injector locations were selected for this purpose. In first case, the injector was located at the centre of the piston head; in the second configuration, the injector was located close to the intake valve at 45° inclination. The valve timing and speed were fixed as x and 1500 rpm, respectively. Fuel injected was 12.5 mg in both cases. The heat release curve thus obtained is shown in Figure 18, and the P-θ curve is shown in Figure 19.

Heat release curves are very similar for both central and angled injections as shown in Figure 18. However, it is seen that heat release peak for central injection is slightly higher than the angled injection; this could be because, in central injection, the tendency for the mixture to become homogenous is higher. As the mixture is more homogeneous, it ignites instantaneously producing a marginally higher heat release peak.

In the pressure plots shown in Figure 19, it was found that the pressure peak for central injection was slightly higher.

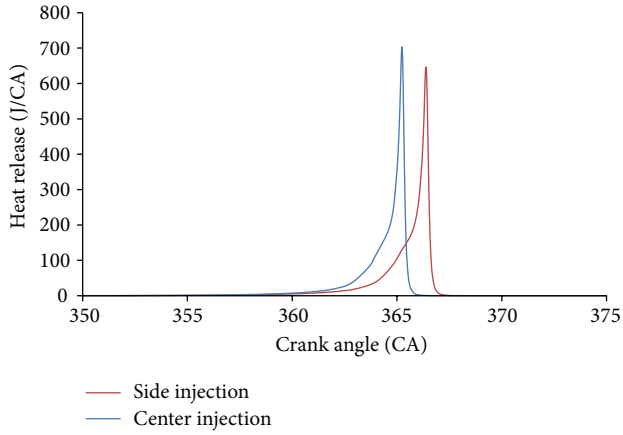

Figure 18: Heat release plots obtained for different injector locations.

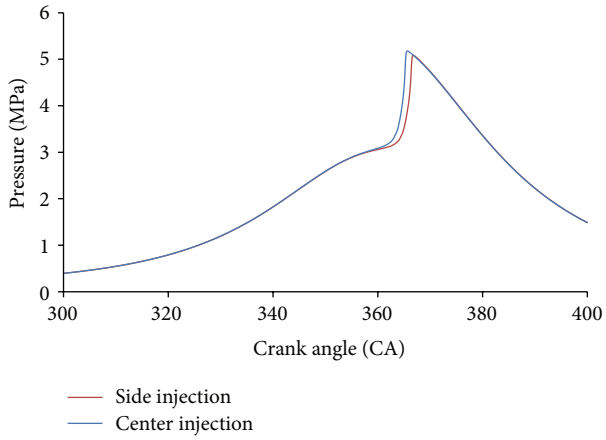

Figure 19: P-θ plots obtained for different injector locations.

This could be because of the heat release peak for central injection, which was slightly higher. This increased heat release may have directly affected the pressure peak.

4. Conclusions

Three-dimensional CFD engine modeling is used to study mixture formation using CONVERGE. Zero-dimensional single zone modeling with detailed reaction mechanism was done to study combustion using CHEMKIN. It was observed that 1500 rpm was able to produce more homogeneous mixture than 1000 and 2000 rpm. It was also observed that regardless of the amount of fuel injected, the mixture formed will be almost homogeneous before combustion. Central injection had more tendency to form homogeneous mixture than side injection. Simulations for different valve lifts indicated that valve lift with highest lift was able to produce more homogeneous mixture. As engine speed increased, the heat release peaks were found to be reducing. Moreover, a shift in the peak was seen with the increase in engine speed. Heat release rates for different valve lifts were found to be negligible. The central injection was found to have better combustion characteristics than side injection.

Acknowledgment

The authors wish to express their gratitude to Dr. Sunil Pandey for his valuable comments and help in performing CHEMKIN simulations.

References

[1] M. Yao, Z. Zheng, and H. Liu, "Progress and recent trends in homogeneous charge compression ignition (HCCI) engines," *Progress in Energy and Combustion Science*, vol. 35, no. 5, pp. 398–437, 2009.

[2] C. V. Naik, W. J. Pitz, C. K. Westbrook, M. Sjoberg, J. E. Dec, and J. Orme, "Detailed chemical kinetic modeling of surrogate fuels for gasoline and application toan HCCI engine," SAE Paper 2005-01-3741, 2005.

[3] H. M. Xu, H. Fu, H. Williams, and I. Shilling, "Modelling study of combustion and Gas exchange in a HCCI (CAI) engine," SAE Paper 2002-01-0114, 2002.

[4] N. P. Komninos, D. T. Hountalas, and D. A. Kouremenos, "Description of in-cylinder combustion processes in HCCI engines using a multi-zone model," SAE Paper 2005-01-0171, 2005.

[5] H. M. Xu, A. Williams, H. Y. Fu, S. Wallace, S. Richardson, and M. Richardson, "Operating characteristics of a homogeneous charge compression ignition engine with cam profile switching-simulation study," SAE Paper 2003-01-1859, 2003.

[6] R. Ogink, "Applications and results of a user-defined, detailed-chemistry HCCI combustion model in the AVL BOOST cycle simulation code," in *Proceedings of the International AVL User Meeting*, pp. 14–15, Graz, Austria, 2003.

[7] N. Milovanovic, R. Dowden, R. Chen, and J. W. G. Turner, "Influence of the variable valve timing strategy on the control of a homogeneous charge compression (HCCI) engine," SAE Paper 2004-01-1899, 2004.

[8] S. M. Aceves, D. L. Flowers, C. K. Westbrook, J. R. Smith, W. J. Pitz, and R. W. Dibble, "A multi-zone model for prediction of HCCI combustion and emissions," SAE Paper 2000-01-0327, 2000.

[9] S. M. Aceves, J. Martinez-Frias, D. L. Flowers, J. R. Smith, R. W. Dibble, and J. F. Wright, "A decoupled model of detailed fluid mechanism followed by detailed chemical kinetics for prediction of iso-octane HCCI combustion," SAE Paper 2001-01-3612, 2001.

[10] S. M. Aceves, D. L. Flowers, C. K. Westbrook, J. R. Smith, and W. J. Pitz, "Cylinder-geometry effect on HCCI combustion by multi-zone analysis," SAE Paper 2002-01-2869, 2002.

[11] O. Roy and G. Valeri, "Gasoline HCCI modelling: an engine cycle simulation code with a multi-zone combustion model," SAE Paper 2002-01-1745, 2002.

[12] S. C. Kong, C. D. Marriot, R. D. Reitz, and M. Christensen, "Modelling and experiments of HCCI engine combustion using detailed chemical kinetics with multidimensional CFD," SAE Paper 2001-01-1026, 2001.

[13] S. C. Kong, C. D. Marriott, C. J. Rutland, and R. D. Reitz, "Experiments and CFD modelling of direct injection gasoline HCCI engine combustion," SAE Paper 2002-01-1925, 2002.

[14] S. C. Kong, R. D. Reitz, M. Christensen, and B. Johansson, "Modelling the effects of geometry-generated turbulence on HCCI engine combustion," SAE Paper 2003-01-1088, 2003.

[15] S. C. Kong, C. D. Marriott, C. J. Rutland, and R. D. Reitz, "Experiments and CFD modelling of direct injection gasoline HCCI engine combustion," SAE Paper 2002-01-1925, 2002.

[16] S. C. Kong and R. D. Reitz, "Modelling the effects of geometry generated turbulence on HCCI engine combustion," SAE Paper 2003-01-1088, 2003.

[17] G. Kontarakis, N. Collings, and T. Ma, "Demonstration of HCCI using a single cylinder four-stroke SI engine with modified valve timing," SAE Paper 2000-01-2870, 2000.

[18] G. Tian, Z. Wang, J. Wang, S. Shuai, and X. An, "HCCI combustion control by injection strategy with negative valve overlap in a GDI engine," SAE Paper 2006-01-0415, 2006.

[19] Y. Li, H. Zhao, N. Brouzos, and T. Ma, "Effect of injection timing on mixture and CAI combustion in a GDI engine with an air-assisted injector," SAE Paper 2006-01-0206, 2006.

[20] "CONVERGE 2.1.0 theory manual," March 2013.

[21] W. C. Reynolds, "The element potential for chemical equilibrium analysis: implementation in the interactive program STAJAN," Tech. Rep. A3391, Stanford University, Stanford, Calif, USA, 1986.

[22] M. Mehl, W. J. Pitz, C. K. Westbrook, and H. J. Curran, "Kinetic modelling of gasoline surrogate components and mixtures under engine conditions," *Proceedings of the Combustion Institute*, vol. 33, no. 1, pp. 193–200, 2011.